Experimental observation of a complex periodic window

D. M. Maranhão,[1] M. S. Baptista,[2] J. C. Sartorelli,[1] and I. L. Caldas[1]

[1] *Instituto de Física, Universidade de São Paulo, Caixa Postal 66318, 05315-970, São Paulo, SP, Brasil*
[2] *Max-Planck Institute für Physik komplexer Systeme, Nöthnitzerstr. 38, D-01187 Dresden, Deutschland*

The existence of a special periodic window in the 2D parameter space of an experimental Chua's circuit is reported. One of the main reasons that makes such a window special is that the observation of one implies that other similar periodic windows must exist for other parameter values. However, such a window has never been experimentally observed, since its size in parameter space decreases exponentially with the period of the periodic attractor. This property imposes clear limitations for its experimental detection.

PACS numbers: 05.45.-a

The emergence of regular behavior is one of the most studied topics in nonlinear dynamical systems. It is known that by the changing of an accessible parameter, chaos [1] and periodic [2] behaviors will be observed.

The expectation of finding stable periodic behavior inside chaotic regions in parameter space depends on the sizes and shapes of the parameter regions, regarded as *periodic windows* (PWs), for which stable periodic orbits (POs) are found. A PW is a region in parameter space that indicates parameter values for which one finds the lowest periodic attractor of period P, plus the period-doubling cascade with attractors of period P^{2n}, with $n \in \mathcal{N}$ [3].

For systems whose chaotic attractors have only one positive Lyapunov exponent as the Chua's circuit, considered in this experiment, a special type of PW, regarded as *complex periodic windows* (CPW), is everywhere observed in parameter space. The appearance of one such window implies in the appearance of an infinite number of self-similar others that appear side by side aligned along a direction. In addition, CPWs have an extended characteristic in the parameter space. They visit large portions of the parameter space, i.e. one can still stay in the same periodic windows even if especial large variations in two control parameters are made. Due to these two characteristics an arbitrary change in only one accessible parameter can replace chaos by periodic behavior, or vice-versa. So, a better understanding of a CPW is relevant to applications that relay either on a robust periodic oscillation, as mechanical machines, or on a robust chaotic system, as chaos-based communication [4].

These CPWs, regarded as *shrimps* [5], were extensively studied in maps [6, 7] and in periodically forced maps [8, 9]. However, only recently these windows were numerically observed in systems of ordinary differential equations [10, 11]. The reason is that the parameter interval length, $\Delta\mathcal{P}$, of a CPW scales exponentially with $-P$, where P is the period P of the lowest-period periodic attractor of the CPW [6]. Since CPWs have usually higher P, they are too tiny to be observed, even though these tiny windows are extended in parameter space.

This exponential scaling clearly imposes limitations to the experimental detection of such a periodic window, and arguably due to that they have never been experimentally reported. However, for the Chua's circuit, it was numerically shown in Ref. [11] that such CPWs possessing a low value for the lowest-period periodic attractor (P=4) exist. This work is dedicated to experimentally report, for the first time, such a CPW.

To certify that we observed a CPW, we show that there exists curves in parameter space where the POs are super-stable, and that these curves cross transversally at least twice, a necessary condition that defines a CPW. These parameter curves are detected by the indirect method of noting the parameter values at which the symbolic sequences, encoding the type of POs existing within the CPW, change.

The well known Chua's circuit is shown in Fig. 1(A). The control parameters are $R_1 = R_{10} - \Delta R_1$ and $R_2 = R_{20} - \Delta R_2$, where R_{10} and R_{20} have fixed values, ΔR_1 and ΔR_2 are varied by precision potentiometers, with steps of $50m\Omega$ and $200m\Omega$, in the ranges $[0, 17]\Omega$ and [1, 5.5]Ω, respectively. We obtained time series by recording the $V_{C_1}(t)$ voltage with a 12 bits ADC at the rate of 400 ksamples/s. All the attractors were reconstructed by Takens method [12] with time-delay $\tau = 45.0$ μs, that corresponds to 18 data points. Then, the reconstructed attractors are made discrete by measuring $V_{C1}(t+\tau)$ when the reconstructed trajectory reaches the section $V_{C1}(t)$=-2.25V in a clockwise orientation. The value of $V_{C1}(t+\tau)$ when the reconstructed trajectory realizes its n-th crossing in this section is denoted by V_{C1}^n.

In Fig. 1(B), we show the parameter space of this circuit. There, filled black circles represent parameter values for which one obtain the lowest period PO. Along the left border between chaos and the PW [parameters indicated by letters "a" within the boxes of Fig 1(B)] in these two PWs, chaos is replaced by a stable (period-3 or period-4) attractor by a tangent bifurcation by increasing ΔR_2. In the other borders, [parameters indicated by letters "b", "c" and "d"], the lowest-period PO inside the PWs bifurcate and chaos (outside the PW) is reached after a period-doubling cascade by modifying ΔR_2.

To illustrate our analysis techniques, we first use a

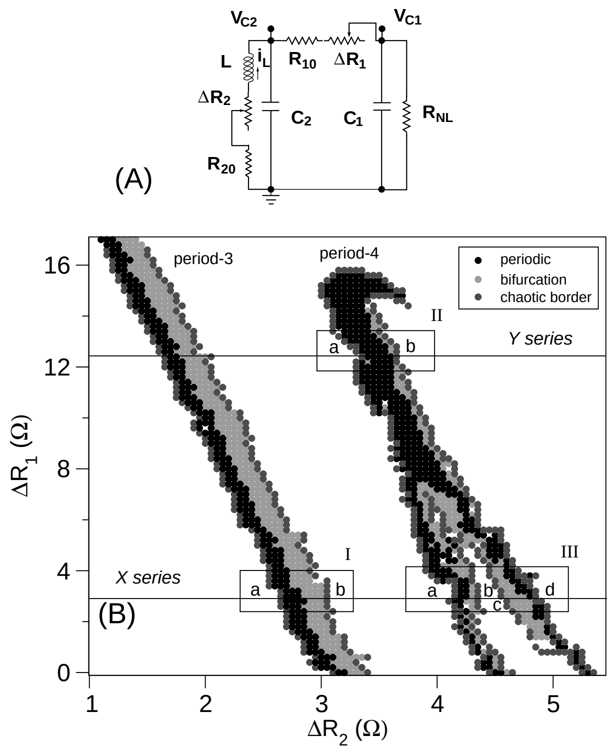

Figure 1: (A) Scheme of Chua's circuit. Their component values are: $R_{10} \approx 1.4k\Omega$, $R_{20} \approx 37\Omega$, $C_1 \approx 4.7$nF, $C_2 \approx 56$nF, $L \approx 9.2$mH. (B) Parameter space for the experimental Chua's circuit showing the period-3 and period-4 windows. Filled black circles represent parameters for which the lowest period POs are observed, filled light gray circles represent the higher period PO that appear by periodic-doubling bifurcations, and filled dark gray circles represent parameters for the closest chaotic attractor to the PWs. The straight lines indicate parameter values for the sets of time series X and Y.

symbolic representation to characterize the lower period POs that appear for the parameters nearby the borders between the PWs and the chaotic regions, indicated by the letters **a**, **b**, **c** and **d**, in the boxes I, II, and III, in Fig 1(B). We use data sets collected varying ΔR_2 along the lines X and Y for $\Delta R_1 = 3.0\Omega$ and $\Delta R_1 = 12.5\Omega$, respectively, as shown in Fig. 1(B).

The symbolic characterization of these POs is done by encoding them by the approach in Ref. [13], using the properties of the nearby chaotic attractors. The return maps of the reconstructed chaotic attractors for parameters in the borders **a**, **b**, **c**, and **d** in box III, are shown in Figs. 2(A-D). These maps as well as the other chaotic attractors at the borders in both period-3 and period-4 windows display return maps typical of either uni (one maximum) or bi-modal (one maximum and one minimum) maps, and they can be partitioned by the critical points. The partitions are in the maximal and minimal points, assigned by V_1 and V_2. So, a trajectory point in the interval $V_{C1} < V_1$ is encoded by '0', a trajectory point in the interval $V_1 < V_{C1} < V_2$ is encoded by '1', and a point in the interval $V_{C1} > V_2$ is encoded by '2'. A stable period-P orbit can be encoded by comparing its mapping with the mapping of the nearby chaotic attractor, and depending on the position of the POs points with respect to the partition points, a PO can be encoded by a sequence $s_1 s_2 \ldots s_P$, where s_i is a symbol of the alphabet $s_i = \{0, 1, 2\}$. For chaotic attractors close to the borders with the period-3 window, in box I, the chaotic returning maps are uni-modal, with only one critical point V_1. In the side **a** of the window, in box I, we obtain the symbolic sequence 101 and in the right side **b**, the sequence 100. All the POs in the left side of this window are encoded by 101 and the ones on the right side by 100. The period-4 POs, in the period-4 window, close to the borders **a**, **b**, **c** and **d**, in box III, [whose return maps can be seen in Figs. 2(A-D), respectively] are encoded by the sequences 1001, 1000, 2000 and 2000, respectively.

In fact, as one varies a control parameter, the symbolic sequence of a stable PO changes if some periodic point crosses a critical point of the return map [14]. This mechanism is responsible for the changes in the symbolic sequences of the stable POs in the period-3 window. There, the symbolic sequence 101 changes to 100 when the PO crosses the critical point V_1.

We name ξ the return map of the closest chaotic attractor to the period-P PO, and $\mathcal{O}$ a stable PO with points $V^1_{C_1}, \ldots, V^P_{C_1}$. Assuming that the return map ξ can be used as an approximation to calculate the first derivative of the orbit points of a PO inside a PW, then the orbit $\mathcal{O}$ is stable if

$$\Delta < 1 \tag{1}$$

with $\Delta = |\prod_{i=1}^{P} \frac{d\xi}{dV^i_{C_1}}|$. If a PO contains a critical point, a point on the extremum of the map, $\Delta = 0$ and we say such orbit is superstable. For parameters ϵ-close to a parameter for which a super-stable PO exists, Eq. (1) is satisfied, which means that it exists a PW in the neighborhood of parameter lines for which $V^i_{C_1} = V_1$.

A similar mechanism governs the changes in the symbolic sequences of the stable POs inside the period-4 region. The difference now is that we have two critical points, V_1 and V_2 which makes Eq. (1) to be satisfied in parameter curves for which either $V^i_{C_1} = V_1$ (which defines the critical curve S_{V1}) or $V^i_{C_1} = V_2$ (which defines the critical curve S_{V2}), or $V^i_{C_1} = V_1$ and $V^i_{C_1} = V_2$. It is typical for this type of CPW that the PW appears not only for the parameter point for which $V^i_{C_1} = V_1$ and $V^i_{C_1} = V_2$, a zero measure point in parameter space, but also along the curves S_{V1} or S_{V2}. These two curves form the spines introduced in Refs. [7, 8].

Three important characteristics grant to this window the status of being a CPW: (i) if there is one CPW, then a countable infinite number of others must exist, with sizes that decreases exponentially [Eq. (2)] as the period of the POs increase; (ii) the two critical curves S_{V1} and S_{V2} cross transversally at least twice. For the parameters

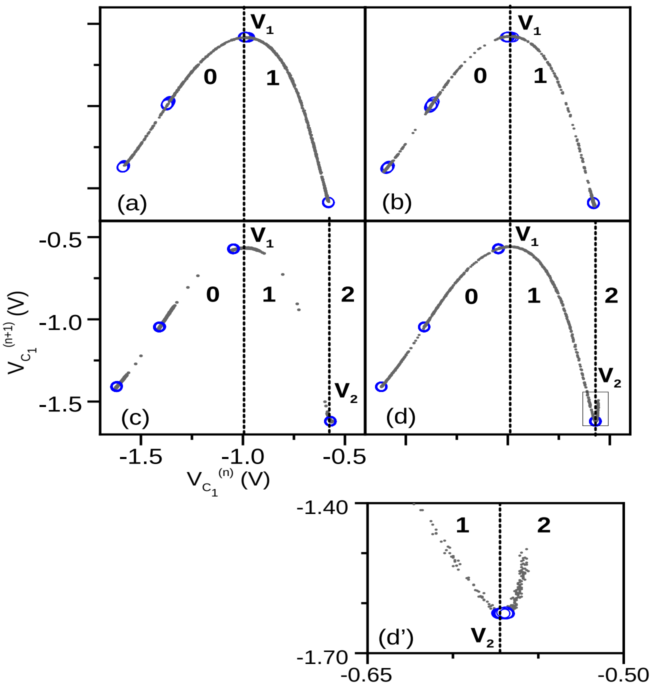

Figure 2: [Color online] Return maps (black points) of the Poincaré section of the chaotic attractors obtained using the parameters indicated by the borders **a**, **b**, **c** and **d** in box III of Fig. 1. We also show the return maps (blue circles) of the periodic attractors obtained for the closest parameters to these borders. The vertical lines, passing through the maximum and the minimum define the partition points. In (d') is shown a zoomed view of the minimum of the return map in (d).

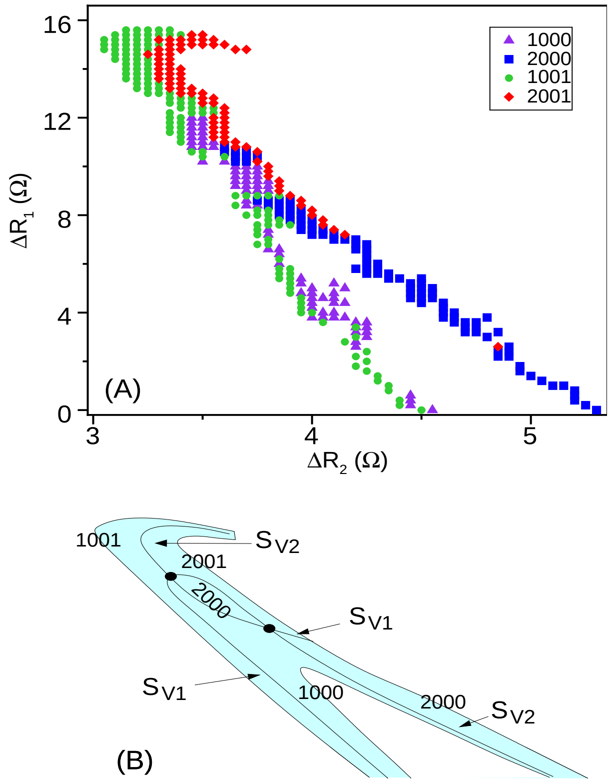

Figure 3: [Color online] (A) The encoding of all the period-4 POs found in the CPW. (B) Sketch of the critical lines (S_{V1} and S_{V2}) structure of the CPW, disregarding the existence of characteristic (iii) that causes the appearance of structures as illustrated in Fig. 4.

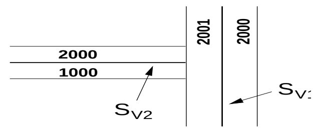

Figure 4: Illustration of the structures that might appear in a CPW due to characteristic (iii).

where the crossings happen, the PO has an orbit point $V_{C_1} = V_1$ and another $V_{C_1} = V_2$; (iii) coexistence of POs with the same period.

Concerning characteristic (i), for quadratic maps one should expect that

$$\Delta\mathcal{P}(P) \propto e^{-\beta P} \tag{2}$$

as shown in Ref. [6], with $\mathcal{P}$ being the parameter interval length of a CPW, and P the period of the lowest-period periodic attractor. Also, from [6], we have that $\beta \cong 2H_T$, where H_T is the topological entropy or Lyapunov exponent of the bordering chaotic region [7, 8]. But, in fact, for flows such as the Chua's circuit containing Shilnikov's homoclinic orbits [15], a two-parameter analysis [16] performed in the neighborhood of this orbit shows that it exists a countable (infinity) number of CPWs that appear side-by-side in parameter space following the same exponential scaling law that describe the appearance of the homoclinic orbits. This exponential scaling law is of the form of Eq. (2) and as shown in Ref. [17], $\beta = \pi\frac{\rho}{\omega}$, with ρ and ω representing the real and imaginary part of the eigenvalues of the focus point associated with the homoclinic orbit responsible for the generation of the many CPWs.

We estimate that for this experimental circuit $\beta \approxeq 2$, in Eq. (2), for a parameter region in the vicinity of the observed period-4 CPW. That means that in order to observe a higher period CPW, with period $P_h = 4^{2n}$, with $n \in \mathcal{N}$, associated with the observed period-4 CPW, we should have a potentiometer with a resolution (step size) of $8\Delta p \exp^{(-2(P_h-4))}$, being that 8 is roughly an average width of the period-4 CPW observed. So, in order to observe a period-8 CPW, we would need a potentiometer with a resolution of about 0.14mΩ, which is much smaller than our experimental resolution. Numerical simulations realized in a similar Chua's circuit, reported in Ref. [11], show that CPWs with attractors of period lower than 4 exist. However, their sizes are of the order of 20 times smaller than a period-4 large CPW, similar to the one observed experimentally. Therefore, for the resolution of our experiment, we do not expect to find the many others numerically found CPWs, but only this "giant" one.

To detect the existence of the critical curves, we search for transitions in the symbolic sequence of the POs closer to the borders between the PW and chaos. In box II, the PO encoded by 1001 at the border **a** changes its encoding to 2001 at the border **b**. So, between these two borders, there is a parameter ΔR_2 for which at least one point of the period-4 orbit is $V^i_{C_1} = V_2$. Thus, within these borders there must exist a curve S_{V2}. In box III, the PO encoded by 1001 (border **a**) changes its encoding to 1000 (border **b**), indicating that within these borders there is a PO that visits the critical point V_1. Thus, within these borders there must exist a curve S_{V1}. In box III, the PO in both borders **c** and **d** are encoded by the symbolic sequence 2000, what suggests that within these two borders there must exist either (or both) curves S_{V1} or S_{V2}.

As we go from one side of the CPW to the other side by changing ΔR_2, for a fixed ΔR_1, the points of the return map of the POs wander along an imaginary smooth curve ξ'. This imaginary curve changes its form smoothly, as we vary ΔR_2. For a ΔR_2 close to a parameter where chaos is found (close to the borders **a**, **b**, **c** or **d**), ξ' resembles the return maps ξ of the chaotic attractors. The curve ξ' can be constructed using all the POs observed in this CPW, for a constant ΔR_1. Then, we estimate the location of the critical points of ξ', which provide us the encoding for the period-4 POs within the CPW, in Fig. 3(A). The curves S_{V1} and S_{V2} are located where two different colors (that describe the different encodings) meet. A curve S_{V1} is the border line between two regions representing different encodings. Either '1001' and '1000', or '2001' and '2000'. A curve S_{V2} is the border line between the regions that encode either '1001' and '2001', or '1000' and '2000'. Note that these curves cross transversally at least twice inside the windows, at the points where the regions that encode the four different types of POs meet. This is characteristic (ii) of a CPW [8]. It can be understood by the way CPWs appear in the parameter space. The process can be described as having a normal PW which contains two curves S_{V1} and S_{V2} that do not cross. One can imagine that both curves have a parabolic shape appearing side-by-side. As one changes a parameter of the circuit, the curve S_{V2} approaches S_{V1} crossing it in at least two points forming a structure similar to the one shown in Fig. 3(B), a sketch of a simplified version of what it could be really happening inside the CPW. There, one sees that some regions in the parameter space that represent POs with some encoding (e.g. '1001') do not border a region with some other encoding ('2000'), except for the point where the curves S_{V1} and S_{V2} cross. And when that happens (excluding the atypical case when the curves are tangent), there has to be at least one more crossing inside the CPW, so that the POs appear side-by-side other allowed POs. The rule is '1001' appears aside '1000', which appears aside '2000', which appears aside '2001', which appears aside '1001'.

Such rule can be apparently violated due to characteristic (iii) that leads to points where two or three different regions meet, as represented in Fig. 4. But note that, in fact, the line S_{V1} does not cross the line S_{V2}, and thus, the rule that describes the crossing between these lines is not violated. Internal noise and parameter fluctuations of the circuit partially destroys the CPW. Adding the fact that we have limitations in our parameter resolution, we do not expect to identify all these fine details of the CPW, but rather a lower resolution picture, in which this rule might be apparently violated.

Acknowledgments We thank the financial support of CNPq, FAPESP, and discussions with R. O. Medrano-T.

[1] M. V. Jacobson, Comm. Math. Phys., **81**, 39 (1981).
[2] J. Graczyk and G. Świątek, Annals of Math. **146**, 1 (1997).
[3] Since the parameter interval occupied by higher-period attractors decreases in a power-law fashion with the period of the attractor, we do not expect to observe the higher-period attractors of a PW, in an experiment. In this work, we only consider the lowest-period periodic attractor in a PW.
[4] M. S. Baptista, E. Macau, C. Grebogi, E. Rosa, and Y.-C. Lai, Phys. Rev. E, **62**, 4835 (2000).
[5] J. A. C. Gallas, Phys. Rev. Lett. **70**, 2714 (1993).
[6] B. Hunt and E. Ott, J. Phys. A: Math. Gen., **30**, 7067 (1997).
[7] E. Barreto, B. R. Hunt, C. Grebogi, and J. A. Yorke, Phys. Rev. Lett. **78**, 4561 (1997).
[8] M. S. Baptista, E. Barreto, C. Grebogi, Int. J. Bifurcation and Chaos, **13**, 2681 (2003).
[9] M. S. Baptista, I. L. Caldas, Chaos, Solitons, & Fractals, **7**, 325 (1996).
[10] C. Bonatto, J. C. Garreau, and J. A. C. Gallas, Phys. Rev. Lett. **95**, 143905 (2005); Y. Zou, M. Thiel, M. C. Romano, Q. Bi, J. Kurths, Int. J. Bifurcation and Chaos, **16**, 3567 (2006); V. Castro, M. Monti, W. B. Pardo, *et al.*, Int. J. Bifurcation and Chaos, **17**, 965 (2007).
[11] M. S. Baptista, *Perturbing non-linear systems, an approach to the control of chaos*, Ph.D. Thesis, Chapter 5, (1996). Download at http://www.teses.usp.br/
[12] F. Takens, *Detecting strange attractors in turbulence. In: Dynamical Systems and Turbulence*, D. A. Rand e L. S. Young (eds.) Springer Lectures Notes in Mathematics, vol. 898, Springer-Verlag, Berlim, 1980.
[13] R. Gilmore and K. W. MacCallum, Phys. Rev. E, **51**, 935 (1995).

[14] N. Metropolis, M. L. Stein, and P. R. Stein, J. Comb. Theor. A, **15** 25 (1973).

[15] A Shilnikov homoclinic orbit is an orbit homoclinic to a saddle-focus point for which $|\rho/\lambda| < 1$, where λ is one real eigenvalue and ρ is the real part of the other two complex conjugate eigenvalues.

[16] P. Gaspard, R. Kapral, and G. Nicolis, J. of Stat. Phys. **35**, 697 (1984).

[17] R. O. Medrano-T., M. S. Baptista, and I. L. Caldas, Chaos, **16**, 043119 (2006).